Renewable Energy 199 (2022) 87–102

Contents lists available at ScienceDirect

Renewable Energy

journal homepage: www.elsevier.com/locate/renene

Data-driven mapping of hourly wind speed and its potential energy resources: A sensitivity analysis

Antonio-Juan Collados-Lara [a,*], Leticia Baena-Ruiz [b], David Pulido-Velazquez [b], Eulogio Pardo-Igúzquiza [c]

[a] Department of Civil Engineering, University of Granada, Water Institute, Ramón y Cajal, 4, 18003, Granada, Spain
[b] Spanish Geological Survey (IGME), CSIC, Urb. Alcázar del Genil, 4. Edificio Zulema, Bajo, 18006, Granada, Spain
[c] Spanish Geological Survey (IGME), CSIC, Ríos Rosas, 23, 28003, Madrid, Spain

ARTICLE INFO

Keywords:
Wind speed mapping
Wind speed energy
Geostatistics
Wind distributions
Granada province (Spain)

ABSTRACT

Renewable energies play a significant role to mitigate the impacts of climate change. In countries like Spain, there is a significant potential of wind energy production which might be a key resource. In this research, we obtain wind power at 80 m height and wind turbine energy (assuming a specific turbine). To achieve this objective we produce an optimal mapping of the hourly "instantaneous surface wind speed" (height 10 m), based on the available data. An extensive region (Granada Province, south Spain) is studied with a spatial resolution of 300 m, during a long period (1996–2016). It allows us to assess the intra- and inter-daily variability of wind energy resources. Several interpolation approaches are tested and a cross validation experiment is applied to identify the optimal approach. The obtained maps were compared with the results obtained in the stations with two common frequency distributions (Rayleigh and Weibull). This is the first time that this sensitivity integrated analysis is performed over an extensive region (12600 km^2) for a long time period (20 years) at fine spatio-temporal resolution (300 m, hourly scale). The results can be very valuable for a preliminary analysis of potential optimal location of wind energies facilities.

1. Introduction

The assessment of wind speed fields and wind speed frequency distribution in specific locations can be very useful for the analyses of different practical problems: design of engineering structure (eg. bridges; [1], data-driven wildfire [2], energy productions [3]. In this research we focused on the analyses of their influence on the potential wind energy production. It is a type of renewable energy, which is gaining significance as a strategic resource to mitigate greenhouse gases emissions and the impacts of climate change. In 2019 Europe had 205 GW of wind energy capacity, which is the 15% of the electricity that the EU-28 consumed in 2019 [4]. Although Germany and Spain have the largest cumulative installed wind energy capacity in Europe, there are still regions in those two countries where, even being the wind conditions optimal, there are not wind energy facilities or there are a reduced number of them [5].

At a global scale, long-term wind speed information is included in two widely used data sources, The Climate Forecast System Reanalysis (CFSR) and the European Centre for Medium-Range Weather Forecasts (ECMWF). The ERA5 is the updated fifth generation of the ECMWF atmospheric reanalysis of the global climate. It replaces the ERA-Interim (ERA-I). ERA5 and ERA-I both have global coverage, however ERA5 provides several advantages over ERA-I. There is a horizontal spatial resolution of 80 km for ERA-I and 31 km for ERA5 and ERA5 provides hourly analysis, while ERA-I provides 6-hourly analysis. ERA5 provides a global product of the history of the atmosphere for the historical period 1979–2020 obtained by combining a forecast model and data assimilation systems to reanalyse past observations. The product has a spatial resolution defined by a mesh with around 31 km of grid side. Another product with higher resolution (around 9 km of grid side) is the ERA5-Land, whose data is a replay of the land component of the ERA5 climate reanalysis with a finer spatial resolution. The analyses of the ERA5-Land, product showed a significant bias in meteorological variables in some regions [6,7]. The CFSR, produced by the National Centers for Environmental Prediction (NCEP), was estimated, designed and executed as a global coupled atmosphere-ocean-land surface-sea ice

* Corresponding author.
E-mail address: ajcollados@ugr.es (A.-J. Collados-Lara).

https://doi.org/10.1016/j.renene.2022.08.109
Received 15 December 2021; Received in revised form 26 July 2022; Accepted 22 August 2022
Available online 1 September 2022

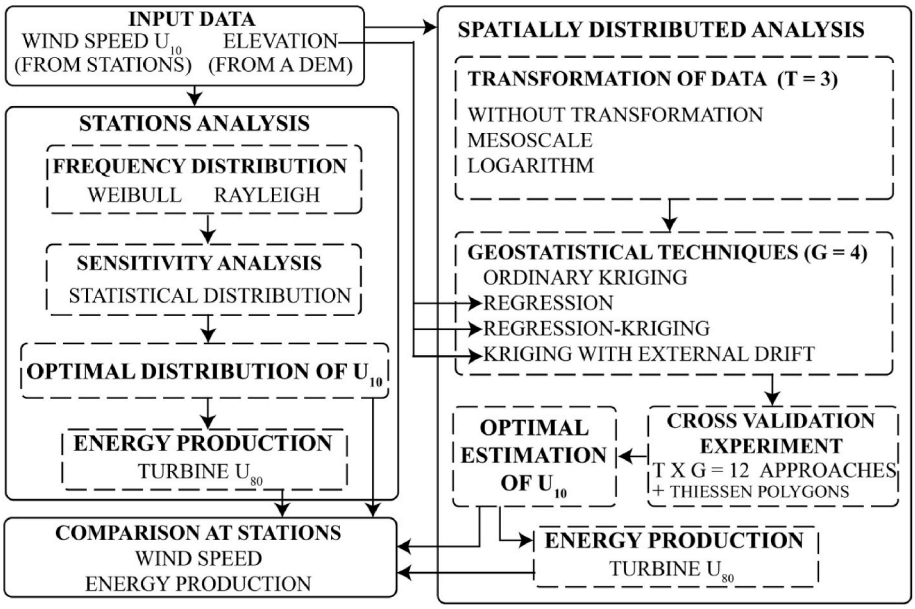

Fig. 1. Flow chart of the proposed methodology.

system to estimate the state of these coupled domains and generates hourly data with a 0.5° horizontal resolution (approximately 56 km) over the period 1979 to 2011 [8]. The CFSR has also been extended as an operational, real time product from 2011 to the present. In the framework of CMIP (https://www.wcrp-climate.org/wgcm-cmip/wgcm-cmip5) and CORDEX (https://cordex.org/) projects, multiples global (with resolution around 200 × 200 km) and regional climatic models (with resolutions between 10 and 50 km) has been employed to perform future predictions and to approximate historical values through reanalyses experiments. Nevertheless, in the literature we find examples where significant bias between the statistics of these climatic data and the local observation is pointed [9,10].

We also find wind speed products with a higher spatial resolution as the Global Wind Atlas (GWA). The version GWA 3.0 is a free, web-based application developed, owned and operated by the Technical University of Denmark (DTU). It combines ERA5 dataset from the for the simulation period 2008–2017 with a Weather Research and Forecasting (WRF) mesoscale model using a grid spacing of 3 km, which is used as input in a microscale modeling system over the globe using the WAsP calculation of local wind climates for every 250 m at five heights (10 m; 50 m; 100 m; 150 m and; 200 m). The high-resolution details of the surface elevation and surface roughness are found to improve the long-term means when compared to observations but a higher resolution does not automatically mean higher quality [11].In countries like Spain, where there is still a significant potential of wind energy production, it might be a key resource if it is used in an optimal way. It requires a rational planning of the wind turbines location (large scale, medium or small scale turbines) based on an optimal mapping of the potential energy resources.

These global products have a coarse spatial resolution (in the case of CFSR and ERA-Interim) and do not represent the temporal (intra- and inter-daily) resolution (in the case of WaSP tool) which are needed for local planning. To this end, long time meteorological measurements at different locations are needed to obtain a distributed map in a large area, although field measurements sometimes has drawbacks related to the lack of data in certain periods or the scarce of meteorological stations in large areas. Then, the wind speed can be also characterized by probability density functions [12] in the stations. The energy production of a turbine can be estimated by integrating the wind speed frequency distribution within the turbine power curve [13], so the selection of the probability density function is an important factor that influences the potential wind energy [14,15]. Over decades, several studies have been conducted to analyze the most suitable probability density functions [16–19] being still a challenging task [20,21]. Although many distribution functions (Gaussian, Gamma, Log Normal, Gumbel) has been proved to fit well the wind speed distribution at different sites, Weibull and Rayleigh distributions are the most widely used [15,16,22]. However, many studies reveal that sometimes the two-parameter Weibull probability function is not quite accurate to fit the wind speed when it takes low values [19,23,24].

Probability functions are useful to assessments in the wind stations but an adequate characterization of the wind requires distributed fields. Geostatistical approaches are useful to generate fields of spatially correlated variables. They use variogram functions to consider the spatial correlation of the experimental data. Some geostatistical approaches allow to consider extra information through means of a secondary variable well-sampled and correlated with the target variable. These multivariate kriging techniques (e.g. regression kriging or kriging with external drift) are useful in the case of data scarcity [25]. Normally, elevation is the most commonly used secondary data to estimate climatic variables. Elevation can also be used to correct wind estimates [26]. Interpolation methods have been previously applied for the assessment of hydrological [eg. snow cover area [27,28] and climatic variables, mainly precipitation and temperature fields [29,30], but also wind speed mapping in some European regions. For example, in Flanders [31] the mean wind speed values were obtained but as the conclusions of this study pointed out, it is not sufficient for accurate wind energy applications. They also pointed the necessity of including additional information, such as seasonal maps and statistics on diurnal variability, to improve the energy map applications for further applications. In Sicily [32], also estimated wind speed using time series that cover a period smaller than 3 years. They pointed out that the size of the available time series is very important to estimate the periodical variability of the wind. The meteorologists generally state that it takes 30 years of data to determine long-term values of weather or climate and that it takes at least 5 years to arrive at a reliable average annual wind speed at a given location.

The aim of this research is to provide an estimation of the instantaneous hourly wind speed and wind potential energy in the province of Granada (south of Spain), which has a wide topographic and climatic variability. As a novelty in this research we analyze the sensitivity of the potential energy production to the interpolation methods [ordinary

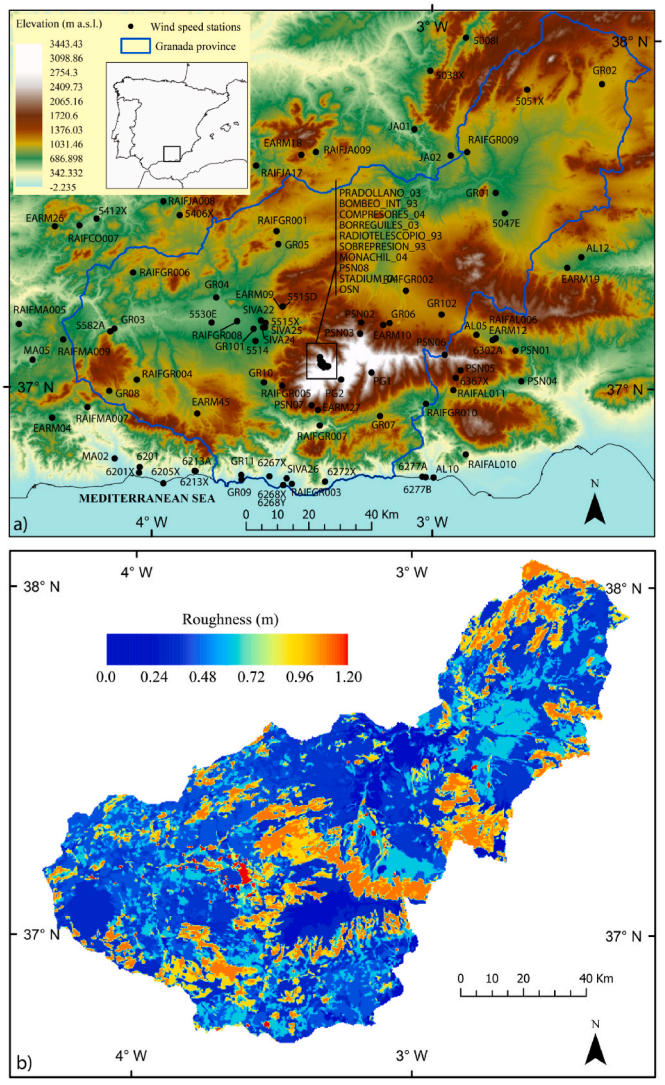

Fig. 2. Case study. Location of the observation points and elevation map (a) and Roughness map (1996–2003) (b).

kriging (OK), regression (R), regression kriging (RK), and kriging with external drift (KED)], the variable interpolated (different transformation functions of the wind speed: U10, U80, and logarithm of U10). These geostatistical approaches to obtain wind fields are also compared to a more simple interpolation method (Thiessen polygons (TP)). We also analyze the sensitivity to the wind speed frequency distribution (Weibull and Rayleigh) to obtain estimations in the data points. This analysis allowed us to obtain potential wind power at 80 m height for an extensive region (the entire province of Granada, 12600 km^2) at fine temporal (hourly) and spatial (300 m) resolutions for a long time period (20 years). We also used a large turbine (80 m height) to calculate the potential energy production of the turbine. The analysis requires an extensive computational effort due to the fine temporal and spatial resolutions and the long period covered. From a practical point of view the results can be very valuable for a preliminary analysis of optimal wind energies facilities location in Granada Province. This work is also useful from the methodological point of view. It includes a general method that can be applied to any case study.

2. Method

A flowchart of the proposed method has been represented in Fig. 1. Our methodology has three main parts: the generation of optimal wind

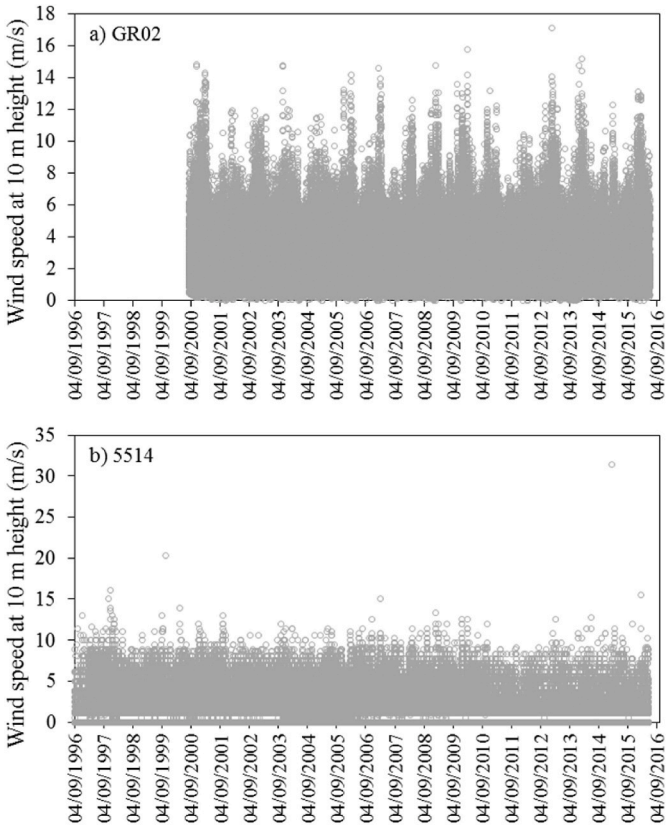

Fig. 3. Hourly wind speed data for the stations GR02 (a) and 5514 (b) in the period September 04, 1996–October 02, 2016.

speed and energy production fields for the entire case study (section 2.1), the calculation of wind speed and energy production in the stations (section 2.2) and the comparison of both results for the stations (section 2.3).

2.1. Optimal interpolation of hourly wind speed. Sensitivity to the applied geostatistical approach and the transformation of the target variable

Wind speed is affected both by local scale phenomena and large scale weather movements. Geostatistical approaches are specially indicated to capture the spatial variability of data through the variogram analysis [33]. Geostatistical estimations will represent the variability of wind speed if the database represents the variability of wind in a region. In this study we elaborated a wind speed database as complete as possible (we used data coming from five public and private agencies and/or research organizations) for the province of Granada (see section 3). We also included elevation as secondary variable (after analyzing several variables as roughness or distance to the coastline) in the approach to take into account topography which is especially relevant in the case study (it varies from 0 to 3479 m.a.s.l) (see section 3).

We tested three different transformations of the wind speed data to obtain the fields. We estimated wind speed at height of 10 m (U10), at 80 m (U80) and the logarithm of U10. The logarithm of the target variable is commonly tested in geostatistical approaches to improve the estimates and the U80 represents the mesoscale wind which is spatially more homogeneous than the surface wind (U10). Both variables are related with Equation (1) [31,34].

$$U_{80} = U_{10} \cdot \frac{\log\left(\frac{80}{rug}\right)}{\log\left(\frac{10}{rug}\right)} \quad (1)$$

where *rug* is the roughness length which can be calculated from land

Table 1
Sill and range of the variograms fitted for the studied variables and its residuals in the regression model with elevation for the different months of the year.

Month	Variograms of the variables						Variograms of the residuals					
	Sill			Range (km)			Sill			Range (km)		
	U10	U80	LN(U10)	U10	U80	LN(U10)	U10	U80	LN(U10)	U10	U80	LN(U10)
1	2.21	5.03	0.71	5.00	2.20	4.50	1.48	3.88	0.65	3.30	3.00	2.10
2	2.82	6.77	0.71	6.00	2.40	3.30	2.09	5.62	0.65	3.90	2.10	4.20
3	2.17	4.88	0.56	3.90	3.00	3.30	1.48	3.86	0.47	4.50	2.40	3.30
4	2.01	4.69	0.56	4.50	3.30	4.50	1.46	3.88	0.49	3.30	2.10	3.30
5	1.56	3.62	0.59	4.20	2.40	1.80	1.08	2.94	0.52	3.00	2.10	5.10
6	1.43	3.46	0.63	0.90	0.90	0.90	1.08	3.01	0.57	1.80	2.10	8.40
7	1.73	3.80	0.87	2.10	1.80	9.60	1.20	3.07	0.80	2.10	1.80	8.40
8	1.93	4.01	0.72	3.30	1.80	9.30	1.06	2.74	0.52	4.20	3.00	2.40
9	1.80	3.71	0.75	3.00	1.80	11.40	1.05	2.63	0.58	5.10	3.30	3.00
10	1.92	3.81	0.73	6.30	4.20	9.60	1.10	2.59	0.55	2.40	2.10	4.50
11	1.81	4.24	0.70	6.00	6.00	9.00	1.24	3.39	0.61	3.30	3.90	5.40
12	1.85	4.10	0.78	3.90	4.20	8.40	1.21	3.21	0.68	4.50	2.40	6.90

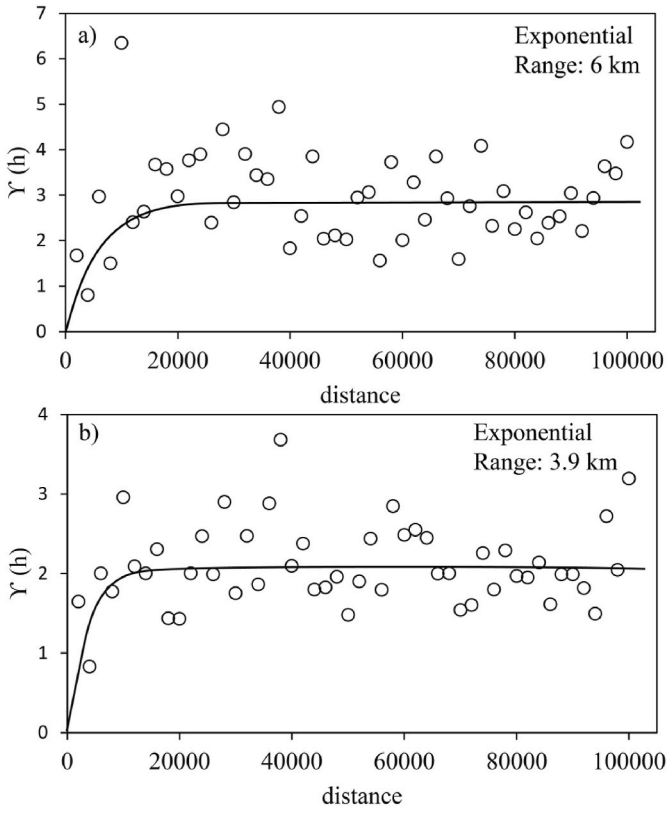

Fig. 4. Variograms fitted for the U10 (a) and its residuals in the regression model with elevation (b) for February.

cover [35].

Note that this formulation may lead uncertainty caused by the complex nature of the wind flow and site conditions such as local meteorology and topography. Data measurements can also include systematic and/or random errors that could be propagated through the modelling [36]. Moreover, the estimation of the roughness length can vary significantly depending on the land cover product use for the calculation [37], although it not necessarily depends on the resolution of the product [38]. Moreover, roughness assignment is not a straightforward task due to it depends on vegetation height and density, among other things, which is not depicted in the land cover resource and might affect to the vertical distribution of the wind speed [39]. Many previous studies have analysed the impact of the uncertainty on the wind resource estimation [36,38].

Table 2
Mean error, mean squared error, and mean standardized squared error of the approaches tested obtained in the cross validation procedure (transformations of the variable and interpolation methods).

Estimation technique	Transformation	ME	MSE	MSSE
Ordinary kriging	–	0.06	3.61	1.85
Ordinary kriging	Mesoscale	0.12	3.88	1.90
Ordinary kriging	Logarithm	−0.56	3.95	0.41
Regression	–	0.17	4.47	3.50
Regression	Mesoscale	0.24	4.63	3.35
Regression	Logarithm	−0.94	5.33	1.16
Regression Kriging	–	0.03	3.46	0.87
Regression Kriging	Mesoscale	0.21	4.50	1.14
Regression Kriging	Logarithm	−0.63	3.84	0.17
Kriging with external drift	–	0.04	3.52	1.57
Kriging with external drift	Mesoscale	0.10	3.78	1.67
Kriging with external drift	Logarithm	−0.56	4.48	0.26
Thiessen polygons	–	0.20	6.23	–

Wind speed is a variable with spatial continuity which changes gradually. Geostatistical approaches take into account the spatial correlation information to estimate fields. Moreover, geostatistical techniques allow us to use a secondary variable to reduce the uncertainties of the estimates. It is also useful when data of the target variable are scarce. The studied area was divided into a finite number of cells of 300 m resolution to obtain hourly wind speed estimates. We estimated the fields in each cell taking as location the coordinates of the centroid of the cell and as elevation the average within the cell (from a 5 m resolution digital elevation model). In this way the estimated fields represent the entire cell and not only the centroid. We used four well known geostatistical approaches (OK, R, RK, and KED) to estimate wind speed fields [25,29]. OK uses only data of the target variable to obtain the estimates and the variogram to quantify the spatial correlation. R uses monthly regression models that relate wind speed and elevation. RK uses the monthly regression models in a first procedure. The second procedure uses the residues of the R to spatially interpolate them using the OK technique. The final estimates are the sum of the R estimate and OK of residuals estimate. In KED the relationship between wind speed and elevation is integrated in the kriging process as external drift that influences the kriging parameters. OK, RK, and KED uses information of spatial correlation of the data. It is quantified through the variogram. We fitted a variogram for each month and variable transformation. In the case of OK the variogram of the estimated variable is used and in the case of RK and KED the variogram is fitted by using the residuals obtained in the monthly regression models using elevation as explanatory variable. We also assessed the TP method to estimate wind speed. It is a simple method which is based on the assumption that measured wind speed at any station can be applied halfway to the next station in any direction,

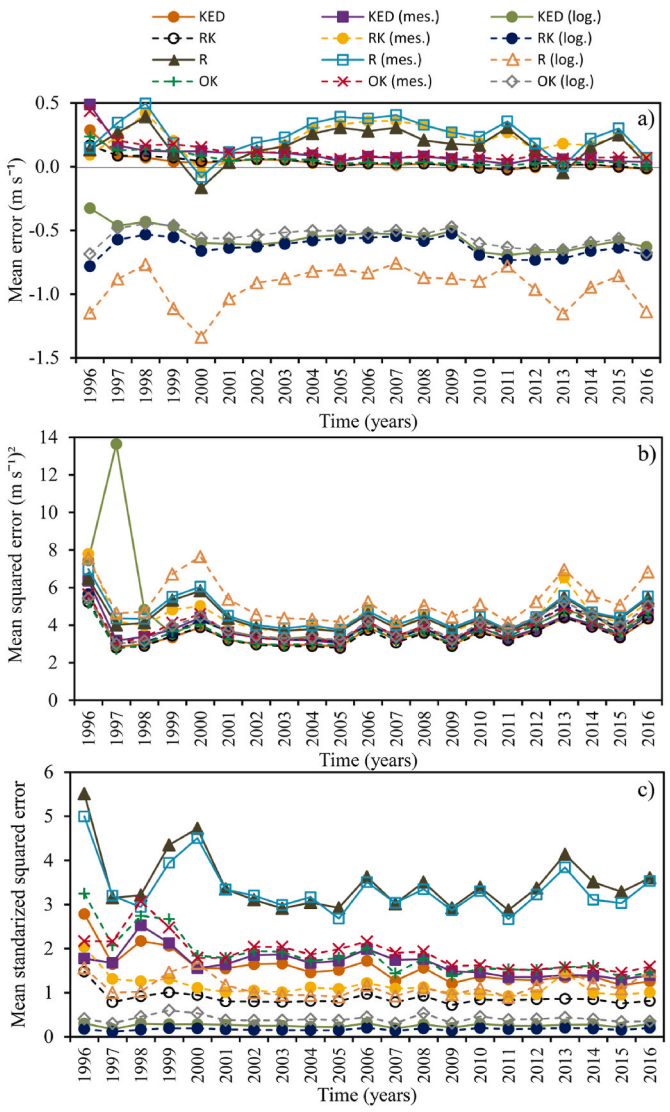

Fig. 5. Results of the cross validation experiment: mean error (a), mean squared error (b), and mean standardized squared error (c).

which means that for any point wind speed is equal to the observed wind speed at the closest station. It allows to know how geostatistical approaches improve the estimations compared to this commonly used method.

The different combinations of geostatistical methods and wind speed transformation of data (12 approaches in total) and the TP method were assessed by using a cross validation experiment. In geostatistics the term "cross validation" [40,33] is generally accepted as the following procedure also known as the leaf-one-out cross-validation: 0) The variogram of the variable of interest (wind speed in our case) is estimated using the complete set of n experimental data, 1) One datum is eliminated from the data set, 2) The rest n-1 data are used to produce an estimate of the variable at the location where the datum was eliminated, 3) The true error incurred in this process is calculated by (Actual Value - Estimated Value) 4) Steps 1 to 3 are repeated for the n experimental data. 5) Cross-validation statistics are calculated by using the n true errors. We compared three statistics obtained from the cross validation experiment: the mean error (ME), the mean squared error (MSE), and the mean standardized squared error (MSSE). The ME is the bias of the estimation, whose value should be around zero. The MSE is the accuracy of the estimate and the value should be as small as possible. The MSSE is the evaluation of how well (statistically) the kriging variance is a realistic measure of uncertainty. Note that MSSE is not obtained for TP because it does not provide variance of the estimation. The value of MSSE should be around 1 if the kriging variance is a good measure of uncertainty.

The selected geostatistical approach in the cross validation experiment is used to estimate wind speed (U10 and U80). The wind power at 80 m height (PU80) can be calculated according Equation (2):

$$PU80 = \frac{1}{2}\rho U80^3 \tag{2}$$

where ρ is the air density.

The wind turbine power can be also calculated from wind speed at the height of the turbine (see Equation (1)) by using the power curve of the turbine. The energy production for the studied period is also obtained taking into account the working time of the turbine. Note that in this work we assumed that the instantaneous hourly value of wind speed represent 1 h to calculate the wind turbine energy. We assume that, in our case study, due to the fine temporal resolution (1 h) the difference between using mean wind speed values or instantaneous wind speed values to calculate energy production are small.

2.2. Mean wind speed and potential energy production in the stations. Sensitivity to the assumed statistical distribution (Rayleigh or Weibull)

The mean hourly wind speed can be calculated from the empirical data although a probability density function is usually fitted. The probability density function (PDF) indicates the probability of observing a wind speed during a fraction of time [14]. In this study we used the Weibull and Rayleigh probability density functions. Note that the wind speed data with values equal to zero were transformed to 0.01 to fit these functions.

The Weibull probability density function is defined by Equation (3).

$$f_W(u) = \left(\frac{k}{c}\right) \cdot \left(\frac{u}{c}\right)^{k-1} \cdot \exp\left[-\left(\frac{u}{c}\right)^k\right] \tag{3}$$

where u is the wind speed at a considered height (U_{10}, U_{80}), $f_W(u)$ is the probability of observing wind speed u (if $u < 0$, $f_W(u) = 0$), c is the scale parameter, and k is the shape factor of the distribution. Different methods can be used to estimate these parameters (graphically through probability plots, or by analytical methods such as least squares or maximum likelihood estimation).

The cumulative probability function ($F_W(u)$) of the Weibull distribution is defined by Equation (4).

$$F_W(u) = 1 - \exp\left[-\left(\frac{u}{c}\right)^k\right] \tag{4}$$

The Rayleigh probability density function is a particular case of the Weibull model when the shape factor c is assumed to be equal to 2. The probability density ($f_R(u)$) and the cumulative distribution ($F_R(u)$) functions of the Rayleigh model are given by Equations (5) and (6) respectively.

$$f_R(u) = \frac{\pi}{2} \cdot \frac{u}{v_{avg}^2} \cdot \exp\left[-\left(\frac{\pi}{4}\right) \cdot \left(\frac{u}{v_{avg}^2}\right)^k\right] \tag{5}$$

$$F_R(u) = 1 - \exp\left[-\left(\frac{\pi}{4}\right) \cdot \left(\frac{u}{v_{avg}^2}\right)^2\right] \tag{6}$$

The mean of the wind speed measurements, Weibull and Rayleigh distributions is calculated following Equations (7)–(9) respectively:

$$u_{avg} = \overline{u} \tag{7}$$

$$\mu_W = c \cdot \Gamma\left(1 + \frac{1}{k}\right) \tag{8}$$

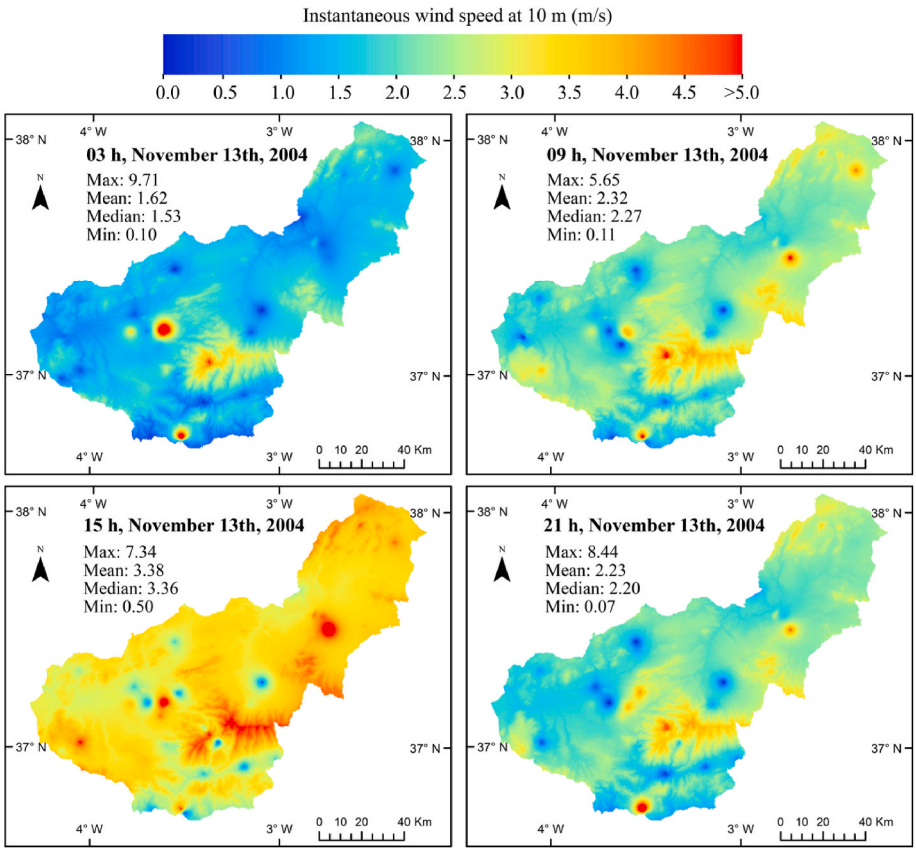

Fig. 6. Instantaneous U10 for the times 03:00, 09:00, 15:00, and 21:00 of November 13th, 2004.

$$\mu_R = \frac{\sqrt{\pi}}{2} \cdot c \tag{9}$$

where N is the number of observing wind speed data; Γ is the gamma function.

The wind power density ($P(u)$) can be assessed by using wind data from measurements or from Weibull and Rayleigh distributions following Equations (10)–(12) respectively.

$$\frac{P(u)}{A} = \frac{1}{2} \cdot \rho \cdot \frac{1}{N} \cdot \sum_{i=1}^{N} u_i^3 \tag{10}$$

$$\frac{P(u)_W}{A} = \frac{1}{2} \cdot \rho \cdot c^3 \cdot \Gamma \cdot \left(\frac{k+3}{k}\right) \tag{11}$$

$$\frac{P(u)_R}{A} = \frac{3 \cdot \sqrt{\pi}}{8} \cdot \rho \cdot c^3 \tag{12}$$

where $\frac{P(u)}{A}$ is the wind power density per swept area of turbine (W/m^2) calculated by using the wind speed measurements, $\frac{P(u)_W}{A}$ is the wind power density per swept area of turbine (W/m^2) calculated by using the Weibull distribution function, $\frac{P(u)_R}{A}$ is the wind power density per swept area of turbine (W/m^2) calculated by using the Rayleigh distribution function, and ρ is the air density (kg/m^3).

Considering a specific wind turbine, the power production can be calculated from the power curve of the turbine.

First of all, we analyze the hourly wind speed measurements available in the stations. Pre-processing tasks were made to original data in order to organize them and remove some irregular values. We calculate the mean hourly wind speed from the empirical data and from the Weibull and Rayleigh distribution functions in order to analyze the suitability of a probability distribution to estimate the mean wind speed and potential energy production.

We also analyze the sensitivity of the wind speed estimation to the statistical characteristics of the time series and the hypothesis assumed about the data frequency distribution.

We considered four statistics to evaluate the performance of the fitted distributions, namely R^2, root mean square error (RMSE), mean absolute percentage error (MAPE) and total absolute bias error (MABE) (Equations (13)–(16)) are used to evaluate the goodness-of-fit of the selected distributions for wind speed data.

$$R^2 = 1 - \frac{\sum_{i=1}^{n}(O_i - E_i)}{\sum_{i=1}^{n}(O_i - \overline{u})} \tag{13}$$

$$RMSE = \sqrt{\frac{1}{n}\sum_{i=1}^{n}(O_i - E_i)^2} \tag{14}$$

$$MAPE = \frac{1}{n} \cdot \sum_{i=1}^{n}\left|\frac{E_i - O_i}{O_i}\right| \cdot 100 \tag{15}$$

$$MABE = \frac{1}{n} \cdot \sum_{i=1}^{n}|E_i - O_i| \tag{16}$$

where n is the number of wind measurements, O_i is the observed wind speed value, E_i is the estimated wind speed value, and $\overline{u}$ is the mean wind speed from observations.

2.3. Comparison of results in the stations vs estimated values in the cells where the stations are located

In those estimation grids where the wind stations are located, we compare the mean wind speed values obtained from the available measurements with those obtained from the complete series of

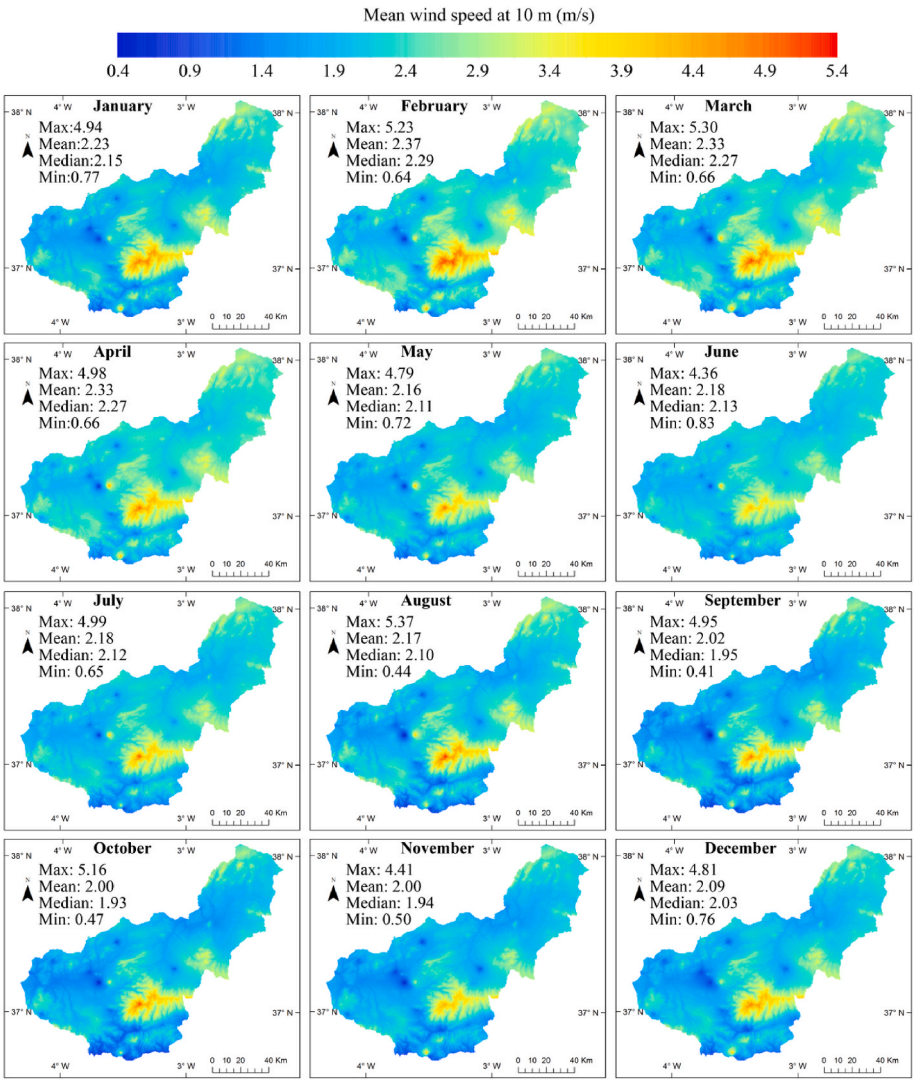

Fig. 7. Maps of mean wind speed at a height of 10 m for the different months of the year.

estimated values in the grid. Note that the estimation values are referred to the each estimation cell and not to the centroid of the cell (see section 2.1). Anyway, we assume that the fine spatial resolution (300 m) used in this work allow to compare the results in the stations with the results in the cells. We assume that the wind speed patterns in the cell represent relatively well each point within it. Considering a specific wind turbine, we also compare the power production calculated from the available measurements with those obtained from the complete series of estimated values in the grid.

In order to compare the mean value of wind speed and wind power density from the empirical data (observed data or estimated series) and from distribution functions (Weibull and Rayleigh) we use the relative difference (δ) (Equation (17)).

$$\delta\,(\%) = \left|\frac{X_{distribution\ function} - X_{empirical\ data}}{X_{empirical\ data}}\right| \cdot 100 \tag{17}$$

where $X_{distribution\ function}$ represents the mean hourly wind speed or the mean wind power density calculated from the Weibull and Rayleigh distribution functions and $X_{empirical\ data}$ represents the mean hourly wind speed or the mean wind power density calculated from the empirical data (observed and estimated fields).

3. Case study and data available

The Granada province is located in southeast of Spain (Fig. 2a). It covers a surface of around 12600 km^2. It has a complex terrain including a wide range of elevations (from 0 to 3479 m a.sl.). Most of the territory has a Mediterranean climate although there is also a mountain climate in the highest parts, and subtropical on the coast.

Currently the province of Granada has 21 wind power plants with a total wind power of 402.21 MW. It represents 51.5% of the total renewable power of the province [41]. Nevertheless, there are still large areas with a high wind potential production where wind power plants could be installed.

Wind data come from different databases from public and private agencies and/or research organizations: Spanish Meteorological Agency (AEMET), Institute for Agricultural and Fisheries Research (IFAPA), Regional Government of Andalusia (REDIAM), the commercial enterprise CETURSA, and Sierra Nevada Natural Park (PNSN).

Data from 94 meteorological stations in the period 1996–2016 were used in this study. Only 55 meteorological stations are located within Granada province. The other 39 stations belong to the surrounding regions out of the Granada province limits (see Fig. 2a). All the meteorological stations were used to estimate the hourly wind speed in the study area within a grid of 300 × 300 m (140395 cells in total) but only the 55 stations within Granada province were used to fit the PDF.

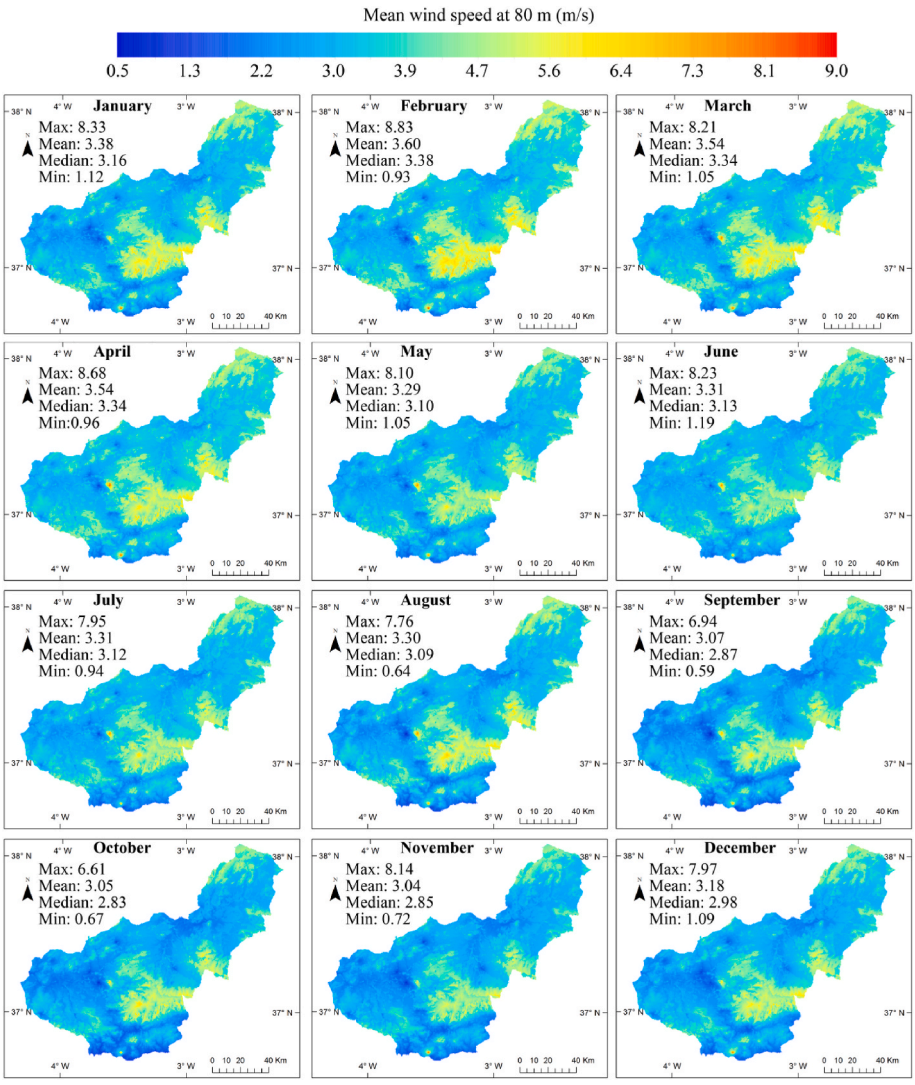

Fig. 8. Maps of mean wind speed at a height of 80 m for the different months of the year.

Table 3
Statistics of goodness of fit for Weibull and Rayleigh distribution functions.

Statistic	Weibull distribution	Rayleigh distribution
R^2	0.95–0.99	0.94–0.99
RMSE	$1.3 \times 10^{-3} - 4.4 \times 10^{-2}$	$3.4 \times 10^{-4} - 3.5 \times 10^{-2}$
MAPE	$7.8 \times 10^{-4} - 6.5 \times 10^{-1}$	$2.9 \times 10^{-4} - 7.2 \times 10^{-1}$
MABE	$8.8 \times 10^{-3} - 1.4 \times 10^{-1}$	$5.5 \times 10^{-3} - 1.4 \times 10^{-1}$

Wind speed is measured at height of 10 m in the meteorological stations. The original data from the different sources were pre-processed in order to organize the data and remove some irregular values. Some of these tasks included to remove certain extremely high values and/or data from periods that presented anomalies (for example calm wind speed for long periods, which might be measurement errors). Most of data suppliers had made a previous validation procedure of the wind variable, so most of data did not have abnormal values. On the other hand, missing values were not considered. The interpolation was made only with the available values for each date.

The 55 stations located within Granada province are located between 10 and 3479 m a.s.l. The data coverage, calculated as the percentage of hours with wind speed data in the analysed period (September 04, 1996–October 02, 2016), is between 6 and 96%. The minimum hourly wind speed in the stations is 0 m/s, and the mean and maximum hourly wind speed varies between 0.48 and 6.34 m/s and 4.19–55.47 m/s respectively. The percentage of data with calm wind (v = 0 m/s) is between 0 and 40% and with low wind speed (below 2 m/s) is between 11 and 98%. In Fig. 3 the data series for the stations GR02 and 5514 are showed (see its location in Fig. 2). The percentage of available data in the studied period for these stations is 77.7% and 72.7% respectively. In the rest of the stations the average percentage of available data is 51.3%.

The wind power potential depends on air density and temperature besides wind speed. The literature typically considers constant (temporal and spatial) average air density and temperature (reference air density, 1.225 kg/m3, corresponding to the sea level and 15 °C) to calculate wind energy production (e.g Refs. [31,42]. In this work, due to the high variation of elevation in Granada province, we considered spatially varying air density and temperature at each location. Air density varies with pressure and temperature following equation (18):

$$\rho = \frac{P}{R \cdot T} \tag{18}$$

where ρ (kg/m^{-3}) is the air density, P (Pa) is the air pressure, R is the gas constant for air (287 J/kg-K), and T is the temperature (K).

We considered a pressure of 101325 Pa and a Temperature of 15 °C for the cells located at sea level and calculated them in the rest of cells according the change of elevation. Note that we assumed the environmental lapse rate (6.5 °C Km^{-1}) [43] to compute air temperature. In the

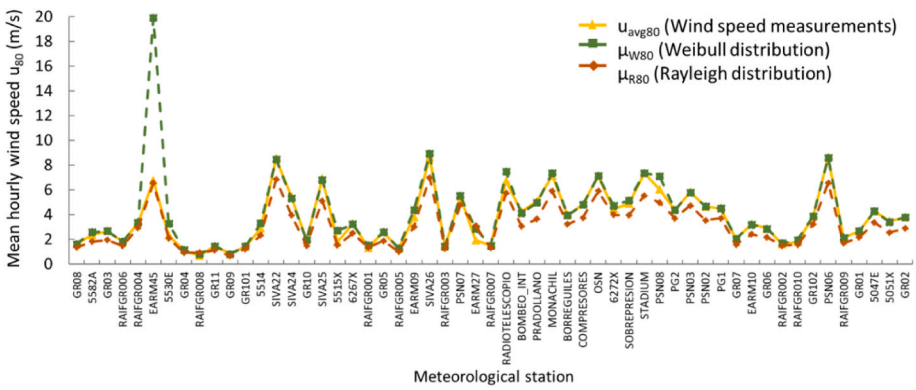

Fig. 9. Mean wind speed (80 m height) calculated from the wind speed measurements and Weibull and Rayleigh distributions.

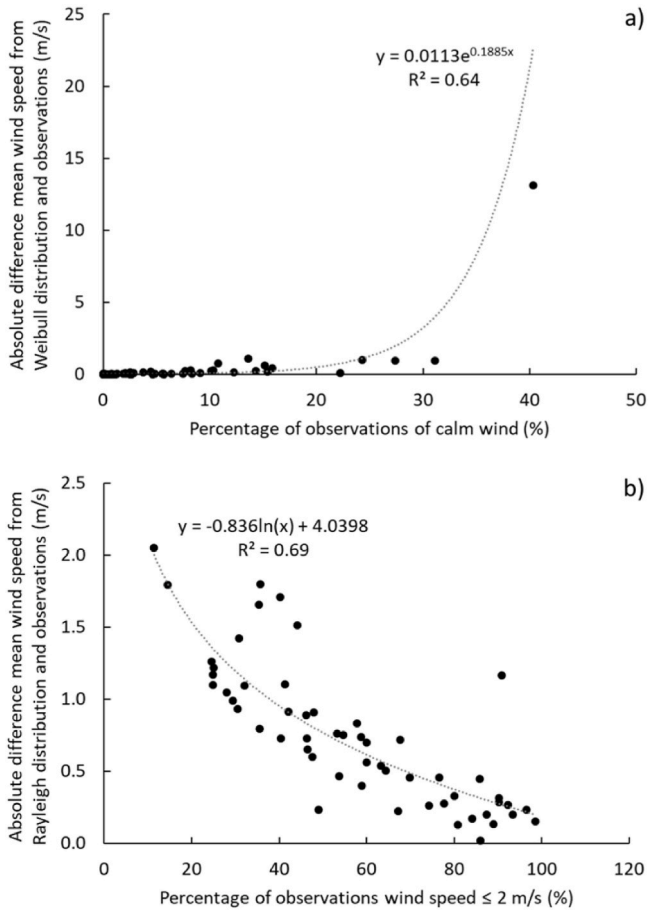

Fig. 10. Relationship between wind calm observations and performance for the Weibull (a) and Rayleigh (b) distribution functions.

case of the pressure, we used the following equation to calculate it at the different elevations from pressure at sea level and the change in elevation:

$$P(z) = P_0 e^{-\alpha Z} \tag{19}$$

where $P(z)$ is the pressure at z elevation, P_0 is the pressure at sea level, and α is a constant defined by equation (20):

$$\alpha = \frac{\rho_0 g}{P_0} \tag{20}$$

where g is the gravity acceleration.

The wind power turbine AW 70–1500 of 80 m hub height from ACCIONA company was considered to calculate the turbine wind power production in the meteorological stations and in all cells within the estimation grid. The turbine has cut-in speed of 3 m/s and cut-out speed of 25 m/s.

Fig. 2b shows the roughness map calculated from Corine Land Cover (CLC) dataset, following the proposal by Ref. [35]. For the studied period we considered two roughness maps from 1996 to 2003 and from 2004 to 2016 because the CLC dataset changed.

4. Results

4.1. Optimal interpolation of hourly wind speed. Sensitivity to the applied geostatistical approach and the interpolated variable

The first step before to the application of the geostatistical approaches was the assessment of the spatial correlation through the calculation of the variogram for the target variable and its transformations. We used an exponential model variogram fitted for each month. In the case of OK the variogram of the estimated variable was used to obtain the variogram and in the case of RK and KED the variogram was fitted by using the residuals obtained in the monthly regression models using elevation as explanatory variable. The sill and the range of the fitted variograms are showed in Table 1. An example of the fitted variogram for the U10 and the residuals of U10 in the regression model is showed in Fig. 4 for the month of February.

The different geostatistical approaches and transformations of variables were tested under a cross validation procedure. We also compared them with the TP estimation method. All the geostatistical approaches proposed in this work provide better performance than the TP method in terms of MSE (see Table 2). In total 12 geostatistical approaches were compared in terms of ME, MSE, and MSSE. The mean values of these statistics for the different years of the studied period (1996–2016) are showed in Fig. 5. In general there are not big differences between the different years. The mean values for the entire period are collected in Table 2. The approaches without variable transformation show better results than the rest for all the geostatistical techniques. The mesoscale transformation is better than logarithm transformation for OK, R, and KED while logarithm transformation is better for RK. The estimation approach with the lower ME and MSE is RK without transformation with 0.03 m/s and 3.46 $(m/s)^2$ but other approaches as OK and KED without transformation show similar results. RK without transformation has also the best MSSE which indicates that the kriging variance is a realistic measure of uncertainty.

RK without transformation of variable is selected to estimate U10. The estimation is done at hourly temporal scale and 300 m spatial resolution for studied period (1996–2016). We generated instantaneous U10 maps each hour for the studied period. An example of these maps is observed in Fig. 6 which represents instantaneous U10 for the times

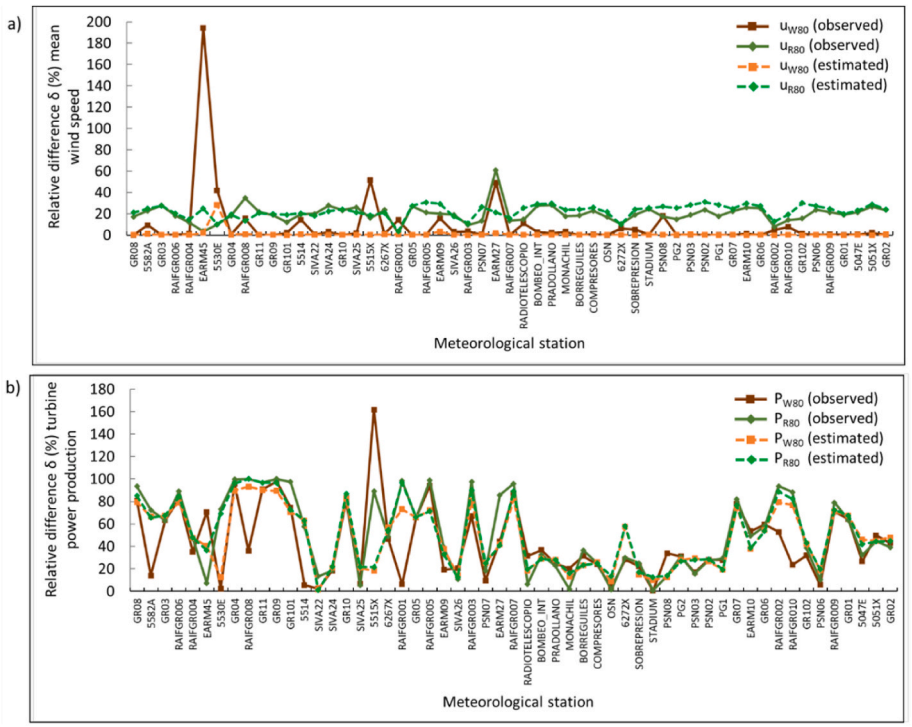

Fig. 11. Relative error in wind speed (a) and turbine energy production (b) calculated from distribution functions and from observed and estimated series.

03:00, 09:00, 15:00, and 21:00 of November 13th, 2004. In general the higher areas show higher values of U10. For this day, mean U10 for the times 03:00, 09:00, 15:00, and 21:00 is 1.62, 2.32, 3.38, and 2.23 m/s. The generated hourly information was also used to obtain average monthly values. The mean U10 in the different months of the year for the studied period is represented in Fig. 7. Higher mean U10 are observed from January to April (winter and beginning of spring) with the highest mean value of 2.37 m/s in February. Lower values are observed from September to December (autumn) with the lowest value of 2.00 m/s in October and November. In general the areas with higher U10 are higher elevation areas (Sierra Nevada and some higher areas of the north of the province) and some coastal areas.

We also obtained mean monthly maps for U80 which refers to the height of the large wind turbines (Fig. 8). We observe a similar distribution than U10. Higher mean U80 are observed from February to April (end of winter and beginning of spring) with the highest mean value of 3.60 m/s in February. Lower values are observed from September to December (autumn) with the lowest value of 3.04 m/s in November. In this case the differences of U80 by elevation are not so higher than for U10 but in general the areas with higher U80 are higher elevation areas too (Sierra Nevada and some higher areas of the North of the province).

4.2. Mean wind speed and potential energy production in the stations. Sensitivity to the assumed statistical distribution (Rayleigh or Weibull)

The frequency distribution can be obtained in accordance with the empirical histogram or assuming a type of distribution function. The most commonly assumed for wind analyses are the Weibull and the Rayleigh distributions. Matlab® code was used to fit the optimal PDF (Weibull and Rayleigh) to both wind data from the 55 meteorological stations and wind estimations in the grid cells where the stations are located. This function uses the maximum likehood method to estimate the parameters of PDF. The goodness of fit statistics of distribution functions (Weibull and Rayleigh) to the data from the 55 stations are summarised in Table 3. All the statistics show that both Weibull and Rayleigh distributions are good enough to fit the wind data in the case study.

Fig. 9 shows the mean hourly wind speed calculated directly from measurements in meteorological stations and by using a Weibull and Rayleigh distribution functions (Equations (6)–(8)). Although the goodness of fit parameters take similar values in both Weibull and Rayleigh distributions, we observe that Weibull distribution usually estimates a mean wind speed similar to the calculated from observations, although in some stations the differences are considerable. The Rayleigh distribution usually underestimates the mean wind speed but these differences between the stations are quite similar.

The discrepancy in the mean wind speed at some sites is due to the distribution of wind speed presents some anomalies. We analyze the time series characteristics that might affect the performance of the Weibull distribution function in terms of mean wind speed. We observe (Fig. 10) that the highest differences in the mean wind speed are related to meteorological stations having a high number of wind data observations of calm wind (u = 0 m/s). The Weibull distribution in those stations also has small shape parameter values and larger scale factor, which results in high mean wind speed. On the contrary, the Rayleigh distribution shows lower differences regarding to the observations when the mean wind speed takes low values (≤2 m/s).

4.3. Comparison of results in the stations vs estimated values in the cells where the stations are located

In those estimation grids (300 m resolution) where the wind stations are located we compare the mean U80 values obtained from the available measurements and the application of distributions functions (Weibull and Rayleigh) with those obtained from the complete series of estimated values (using RK) in the grid (Fig. 11a). Assuming a turbine AW 70–1500 of 80 m height, we also compare the potential energy production obtained from the available measurements with those obtained from the complete series of estimated values in the grid (Fig. 11b).

The analysis of the relative difference in the mean wind speed and energy production calculated by using the distribution functions (Weibull and Rayleigh) and the empirical data (observations in meteorological stations and RK estimations) yields different results. The mean

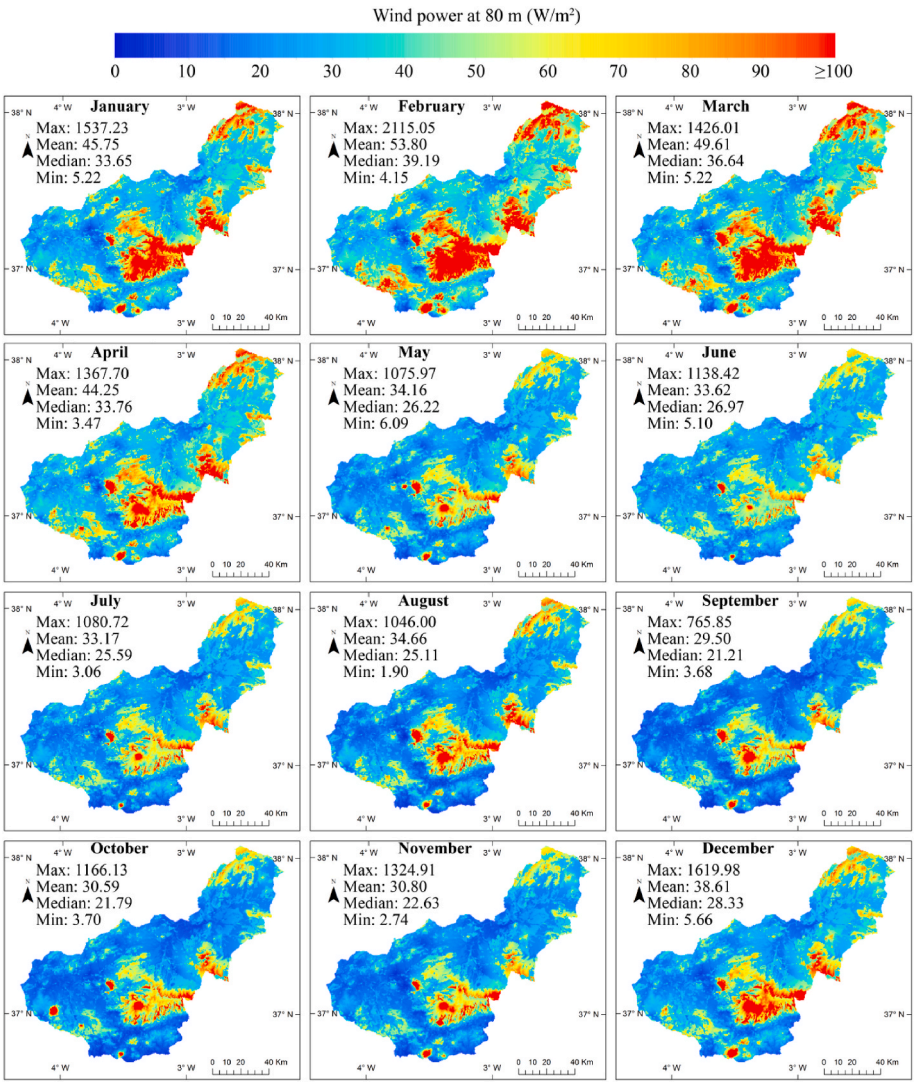

Fig. 12. Maps of mean wind power at a height of 80 m for the different months of the year.

wind speed and energy production calculated from Weibull distribution are more similar to the RK estimations. However, the differences between using observation or estimations and the Rayleigh distribution to calculate the mean wind speed and energy production are not significant.

The distributions functions used have a good fit to the data (RMSE is below 0.044 m/s (see Table 3)). RK have also a good performance in the cross validation experiment (RMSE 1.87 m/s (see Table 2)). Note that the procedure to obtain RMSE in both approaches (distributions and RK estimation) is different and cannot be compared. In the cross validation procedure each experimental data is dropped from the experimental data set in turn and it is calculated from the remaining experimental data. However all the data are used to fit the Weibull and Rayleigh functions. Note that the geostatistical estimations use the available data as outputs when they are available. If we do not use the cross validation experiment to assess the performance, we would obtain a RMSE of 0.0 for RK.

We observe similar differences of the distributions with the data and the estimations (Fig. 11). On the other hand, the RK estimations allow us to obtain spatio-temporal distributed wind fields (section 4.1) while distributions functions allow to obtain them only at stations (section 4.2). The spatio-temporal distributed wind fields are used to obtain potential energy production maps in the following section.

4.4. Estimation of the potential energy production maps

The U80 data are used to calculate wind power at 80 m height (PU80). Due to variability of elevation in Granada province (from 0 to 3479 m a.s.l.) we used a variable value of air density instead of considering the standard value of 1.225 kg/m^3 to calculate PU80. PU80 maps (Fig. 12) gives an idea of the potential optimal location of wind energies facilities in Granada Province. Note that these maps do not depend on the kind of wind turbine, and therefore, they could be used for different companies and administrations. From January to April the mean PU80 in the Granada province is between 44.25 and 53.80 W/m^2 but it can be very variable depending on the location (minimum of 3.47 and maximum of 2115.05 W/m^2). The rest of the year PU80 is lower (mean around 30 W/m^2) with a high variability depending on de area (minimum of 1.90 and maximum of 1609.98 W/m2). In general the variability in P80 is associated to elevation but some areas located in the cost present also high values of PU80.

The PU80 maps represent the potential power of wind but depending on the turbine used the effective power will be different. We also used the wind power turbine AW 70–1500 of 80 m height from ACCIONA company to calculate wind turbine power at 80 m height (TPU80) (see Fig. 13). In this case the TPU80 is expressed in KW because the geometrical characteristics of the turbine are known. We also used the operational characteristics of this turbine to calculate the percentage of

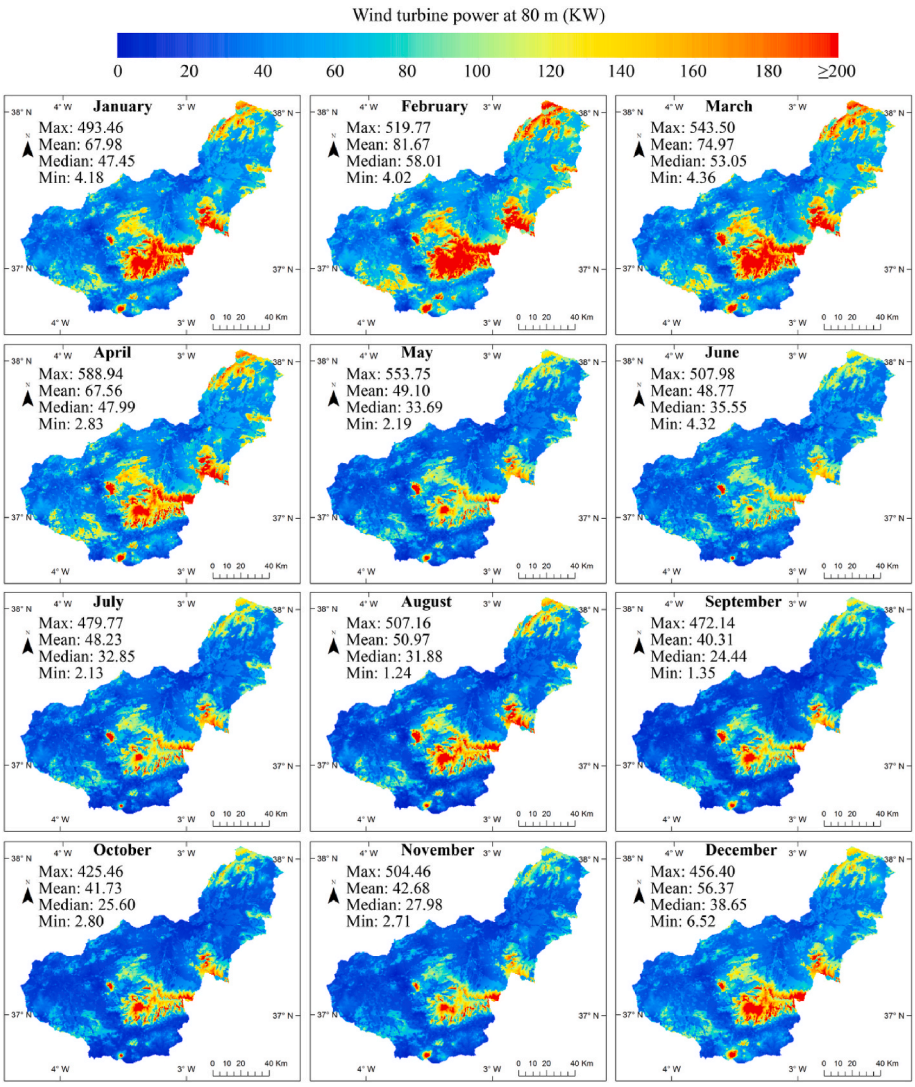

Fig. 13. Maps of mean wind turbine power at a height of 80 m for the different months of the year.

time that the turbine would have been working (3 m/s < U80 < 25 m/s) in the studied period (see Fig. 14). the minimum value in the province is 5.0% and the maximum 99.9%. Higher elevation areas show a higher working time of the turbine. The mean working time as percentage for the province of Granada is 46.9%. We also calculated the wind turbine energy at 80 m height (TEU80) that the selected turbine would produce in the studied period (September 04, 1996–October 02, 2016) in each pixel of the estimation grid (see Fig. 15). The mean TEU80 for Granada province vary from 606.5 MWh (September) to 1115.6 MWh (March).

5. Discussion

This work provides wind, potential energy production, and energy production for specific turbine fields in the province of Granada (12600 km^2). We used a long period 1996 to 2016 (20 years) and high temporal (hourly) and spatial (300 m) resolutions. Others works assessed energy production from wind in regions as Sicily (25711 km^2) [32] or Flanders (13.625 km^2) [31]. Cellura et al. [32] used 29 wind stations (1.1 stations/1000 Km^2) for a period of 3 years and [31] used 45 wind stations (3.3 stations/1000 Km^2) for a period of 5 years. In this work we used 7.5 stations/1000 Km^2 and a period of 20 years. With respect the temporal resolution Cellura et al. [32] used hourly data (as in our study) and [31] used daily data. Moreover, these previous studies obtained an average wind speed map which is not sufficient for wind energy applications. In this study we presented monthly maps but the generated product allows to study daily variability because it is generated at hourly temporal resolution.

From the, methodological point of view we also included transformation of the target variable to assess the performance of the geostatistical approaches. The previous works used directly the target variable. We also used a variable air density depending on elevation to obtain the energy production. Note that our case study has a variation of elevation of around 3500 m and the air density is a key issue for energy production [31]. did not use a variable air density but in this case is justified because the elevation change in Flanders is minimal. However, the procedure used in this work is recommended for cases studies as Sicily which has a similar variation in elevation.

We also compared mean values of our product with the ERA5-Land product (spatial resolution around 10 km) and the Global Wind Atlas (250m spatial resolution) and calculated the correlation coefficient of these maps (Fig. 16). ERA5-Land is not correlated with our product ($R^2 < 0.15$) and the GWA shows a moderate correlation ($R^2 = 0.25$). We also obtained the R^2 of mean wind speed with elevation in the station locations for the four sources of information (data, RK estimation, GWA, and ERA5-Land). The R^2 is respectively 0.47, 0.66, 0.45, and 0.21. The data, RK estimation and GWA show a correlation with elevation. However ERA5-Land does not capture the local patterns of winds due to elevation. Note that ERA5-Land is a replay of the land component of the ERA5 with

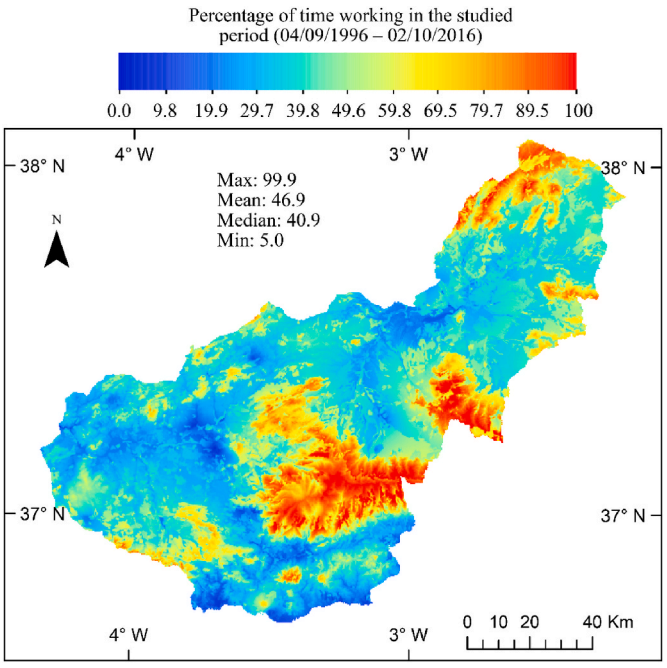

Fig. 14. Percentage of time that the turbine AW 70–1500 of 80 m height from ACCIONA company would have been working (3 m/s < U80 < 25 m/s) in the studied period (September 04, 1996–October 02, 2016).

a finer spatial resolution and the calculation resolution of ERA5 is 30x30 Km which seems not enough to capture the local wind patterns. Our case study has an important variation in elevation (from 0 to 3479 m.a.s.l) and ERA5-Land does not show higher wind speed for the higher areas. Others authors also pointed that ERA5 underestimates wind speeds, especially in mountainous areas [44]. ERA5 is a reanalysis product and it is well known that biases in observations and models can introduce spurious variability and trends into reanalysis output. On the other hand, GWA is quite correlated with elevation and the map is similar to our product. We also calculated the errors of the three products with respect the mean values of the data for each station (see Table 4). We confirmed that the ERA5-Land performance (RMSE = 2.37 m/s) is not enough to capture the local patterns of our case study. GWA shows an acceptable performance (RMSE = 1.54 m/s) but overestimate wind speeds (especially for higher elevations) and RK estimation shows the best results (RMSE = 0.66 m/s). Note that the database used for this study is as complete as possible (we used data coming from five public and private agencies and/or research organizations). On the other hand, our product provides hourly estimations for a long period that can be used for several applications (wind power, hydrology, and risk analysis) and the GWA is a map which is not variable in time.

The obtained wind fields in the pixel where the stations are located were also compared to the wind speed and energy production in the stations showing similar results. Note that in general geostatistical estimations generate smoothed fields. We also included a sensibility analysis to the distribution function used to fit the observations in the stations.

Regarding the suitability of fitting a probability function to the observations, the results highlight that Weibull distribution is more appropriate than Raileigh distribution to estimate mean wind speed, although the mean wind speed of Weibull distribution depends on the shape of the wind data distribution. Several previous works revealed that the two-parameter Weibull distribution is not appropriate for properly fitting wind data of low wind speed [15, 23,24]; Ounis and Aries 2020). A wind speed distribution with high frequencies of low wind speed is related to smaller value of the shape factor k in the corresponding Weibull distribution. The results show that the relative difference and absolute difference in the mean wind speed between the Weibull distribution and observations increase when the wind speed measures have a higher percentage of calm wind. Similar findings have also been obtained in previous works [45].

When we compare the mean values of the wind speed calculated by using the geostatistical approaches and by using Weibull or Rayleigh distribution functions, we observe that the estimations usually smooth the wind speed producing lower mean values. However geostatistical approaches allow to obtain spatially distributed fields (in this case with 300 m spatial resolution) and the use of distribution functions in each station only allow to obtain energy production in these stations. The availability of spatio-temporal maps of wind speed and potential energy production is a key issue for local and regional administrations and wind energy companies.

5.1. Hypothesis and assumptions

Although we have demonstrated the utility of the proposed approach for mapping wind fields and potential energy production, we want to highlight some hypothesis, and assumptions that could be addressed in future research.

- Note that geostatistical approaches incorporates the spatial variability of data to the estimation. If the database does not represent the spatial patterns of wind of the area, the errors will be propagated to the estimations. In this work we used a wind speed database as complete as possible (we used data coming from five public and private agencies and/or research organizations) for the province of Granada. However in some areas the density of data is low. The estimation in these areas has a higher level of uncertainty.
- Geostatistical approaches do not incorporate physical laws in the estimations. Hence mass and energy balance is not considered in the generated fields.
- In this paper the distribution functions Weibull and Rayleigh have been used to fit the hourly wind speed data at all meteorological stations and grid cells. Other distributions [46] could be more appropriate in some locations of the case study.
- Note that the transformation of the U10 into U80 might lead uncertainty in the use of the roughness length, which is not considered in this paper, but it could be made in future works. Moreover, the effect of other terrain local features on the vertical distribution of wind is not considered in this paper, which would require a detailed analysis.
- Although the literature typically considers constant annual average air density [31] and we considered a spatially varying air density according the elevation, we assumed that the pressure at sea level and temperature are 101325 Pa and a 15 °C respectively. We also assumed that the temperature lapse rate is constant and equal to the environmental (6.5 °C Km^{-1}). Future works could also explore the seasonal variation of air density [42].
- Although potential wind power has been calculated, a specific wind turbine has been considered to calculate energy production. An optimum wind turbine could be analysed for each location in Granada province.
- Although a fine temporal resolution is used, we assumed that the instantaneous hourly value of wind speed (instead mean value) represents 1 h to calculate the wind turbine energy.
- The optimal location of the wind turbine would also include others criteria (protected areas, environmental impacts, etc.) which were not considered in this study.
- This work is focused on potential energy resources and it does not analyze extreme wind values. Extreme winds are among the most damaging historically over Europe [47] and could be analysed in future works

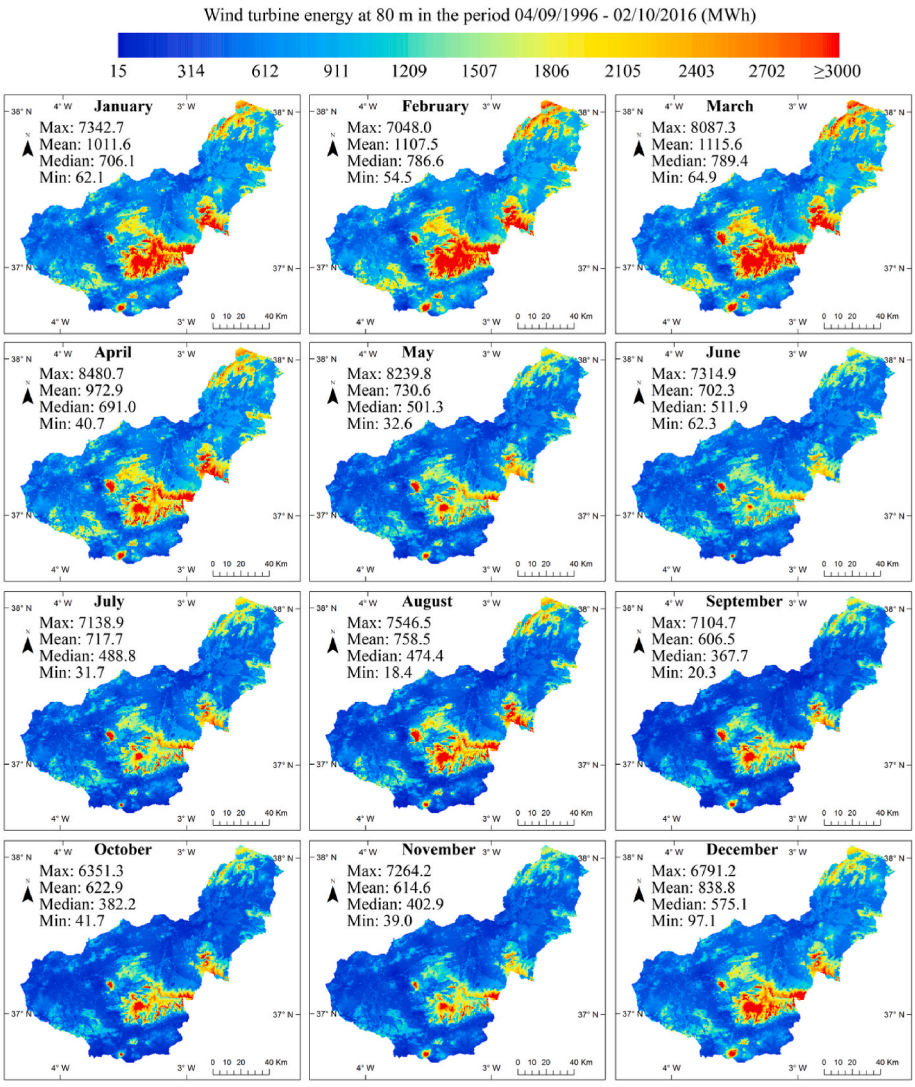

Fig. 15. Maps of wind turbine energy at a height of 80 m for the different months of the year in the period September 04, 1996 to October 02, 2016.

6. Conclusions

In this work we generated a product which is very valuable for a preliminary analysis of potential optimal location of wind energies facilities in Granada Province. We obtained optimal wind and potential energy fields for a 20 years period with hourly temporal resolution and 300 m spatial resolution. We compared 12 geostatistical approaches which include four estimation techniques (OK, R, RK, KED) and three transformation of the target variable. The RK technique without transformation of variables showed the best results in the cross validation experiment.

The wind and energy production fields were compared to the obtained in the stations by using distribution functions (Weibull and Rayleigh). Both showed similar results but the geostatistical approaches provided slightly smoothed values. However these differences are not important if we take into account that the geostatistical approaches allow us to obtain the wind resource in a distributed way for all the Granada province and not only for the stations. It is a key issue for the assessment of optimal location of wind energy facilities.

Compared to previous works that intends to map the wind energy resource, this paper includes several advantages. The studied period is longer and the number of data is higher.It contributes to a better characterization of the saptio-temporal variability of wind. We also included different transformations of the target variable for geostatistical assessment. The obtained product allow to assess the intra- and inter-daily variability and not only the mean values for the entire period studied.

This work is useful from the methodological point of view. It includes a general method that can be applied to any case study. The paper also provides a very useful product to assess the optimal location of wind energy facilities in the province of Granada.

Funding

This research was partially supported by the research project SIGLO-AN (RTI2018-101397-B-I00) from the Spanish Ministry of Science, Innovation and Universities (Programa Estatal de I + D + I orientada a los Retos de la Sociedad) and the Next Generation EU Recovery Funds within the framework of the project C17.i7.CSIC – CLI 2021-00-000. It was also partially supported by the Regional Ministry of Economic Transformation, Industry, Knowledge and Universities of the Regional Government of Andalusia through the postdoc program of the Andalusian Plan for Research Development and Innovation (PAIDI 2021) (POSTDOC_21_00154, University of Granada, Antonio-Juan Collados-Lara). Funding for open access charge: Universidad de Granada/CBUA.

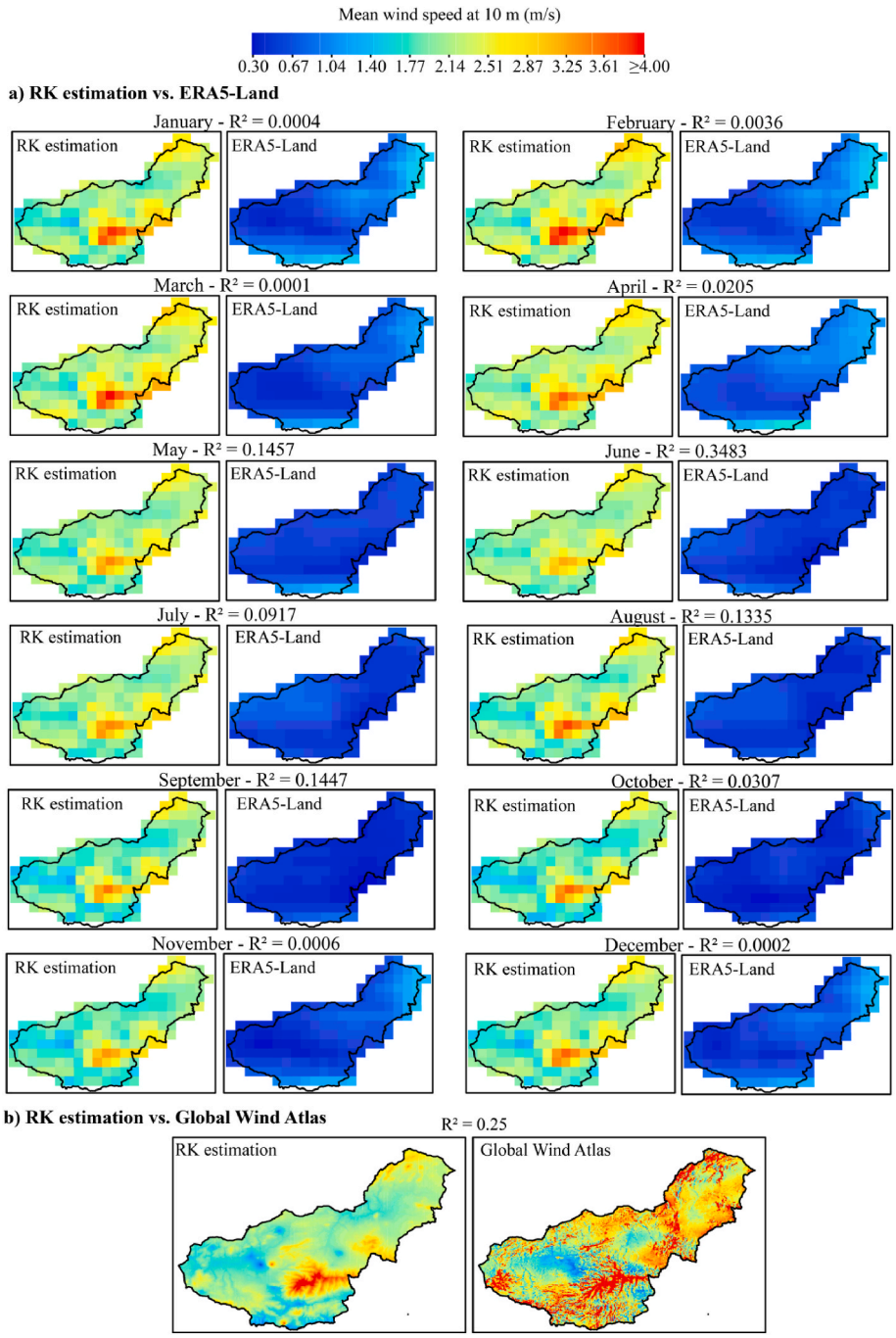

Fig. 16. Comparison of the RK estimation generated in this study with ERA5-Land (a) and the Global Wind Atlas (b).

Table 4
Mean error, mean squared error and root mean squared error of the three products (RK estimation, GWA, ERA5-Land) in the comparison with the mean values of wind speed at the stations.

	RK estimation	GWA	ERA5-Land
ME (m/s)	0.02	−0.47	1.60
MSE $(m/s)^2$	0.43	2.37	5.62
RMSE (m/s)	0.66	1.54	2.37

CRediT authorship contribution statement

Antonio-Juan Collados-Lara: Investigation, Conceptualization, Data curation, Methodology, Software, Validation, Visualization, Writing – original draft, Writing – review & editing. **Leticia Baena-Ruiz:** Investigation, Conceptualization, Data curation, Methodology, Software, Validation, Visualization, Writing – original draft, Writing – review & editing. **David Pulido-Velazquez:** Investigation, Conceptualization, Methodology, Supervision, Writing – original draft, Writing – review & editing. **Eulogio Pardo-Igúzquiza:** Investigation, Conceptualization, Methodology, Supervision, Writing – original draft, Writing – review & editing.

Declaration of competing interest

The authors declare that they have no known competing financial interests or personal relationships that could have appeared to influence the work reported in this paper.

Acknowledgments

We would like to thank the Spanish Meteorological Agency (AEMET), Institute for Agricultural and Fisheries Research (IFAPA), Regional Government of Andalusia (REDIAM), the commercial enterprise CETURSA, and Sierra Nevada Natural Park (PNSN) for the wind speed data provided.

References

[1] T. Tao, H. Wang, C. Yao, X. He, A. Kareem, Efficacy of interpolation-enhanced schemes in random wind field simulation over long-span bridges, J. Bridge Eng. (2018), https://doi.org/10.1061/(asce)be.1943-5592.0001203.
[2] O. Rios, W. Jahn, E. Pastor, M.M. Valero, E. Planas, Interpolation framework to speed up near-surface wind simulations for data-driven wildfire applications, Int. J. Wildland Fire (2018), https://doi.org/10.1071/WF17027.
[3] Y. Feng, L. Que, J. Feng, Spatiotemporal characteristics of wind energy resources from 1960 to 2016 over China, Atmosp. Ocean. Sci. Lett. (2020), https://doi.org/10.1080/16742834.2019.1705753.
[4] WindEurope, Wind energy in Europe in 2018, Trends Stat. (2019). Available online: https://windeurope.org/wp-content/uploads/files/about-wind/statistics/WindEurope-Annual-Statistics-2018.pdf. (Accessed 21 January 2020).
[5] M.D. Leiren, S. Aakre, K. Linnerud, T.E. Julsrud, M.R. Di Nucci, M. Krug, Community acceptance of wind energy developments: experience from wind energy scarce regions in Europe, Sustainability (2020), https://doi.org/10.3390/su12051754.
[6] T. Hong, H. Li, M. Chen, Comprehensive evaluations on the error characteristics of the state-of-the-art gridded precipitation products over jiangxi province in 2019, Earth Space Sci. (2021), https://doi.org/10.1029/2021EA001787.
[7] Z. Wu, H. Feng, H. He, J. Zhou, Y. Zhang, Evaluation of Soil Moisture Climatology and Anomaly Components Derived from ERA5-Land and GLDAS-2.1 in China, Water Resources Management, 2021, https://doi.org/10.1007/s11269-020-02743-w.
[8] S. Saha, S. Moorthi, X. Wu, J. Wang, S. Nadiga, P. Tripp, D. Behringer, Y.T. Hou, H. Y. Chuang, M. Iredell, M. Ek, J. Meng, R. Yang, M.P. Mendez, H. Van Den Dool, Q. Zhang, W. Wang, M. Chen, E. Becker, The NCEP climate forecast system version 2, J. Clim. (2014), https://doi.org/10.1175/JCLI-D-12-00823.1.
[9] E. Pardo-Igúzquiza, A.J. Collados-Lara, D. Pulido-Velazquez, Potential future impact of climate change on recharge in the Sierra de las Nieves (southern Spain) high-relief karst aquifer using regional climate models and statistical corrections, Environ. Earth Sci. (2019), https://doi.org/10.1007/s12665-019-8594-4.
[10] A.J. Collados-Lara, D. Pulido-Velazquez, E. Pardo-Iguzquiza, A statistical tool to generate potential future climate scenarios for hydrology applications, Sci. Program. (2020), https://doi.org/10.1155/2020/8847571.
[11] R. McKenna, S. Pfenninger, H. Heinrichs, J. Schmidt, I. Staffell, C. Bauer, J. Wohland, High-resolution Large-Scale Onshore Wind Energy Assessments: A Review of Potential Definitions, Methodologies and Future Research Needs, Renewable Energy, 2022, https://doi.org/10.1016/j.renene.2021.10.027.
[12] N. Kirchner-Bossi, R. García-Herrera, L. Prieto, R.M. Trigo, A long-term perspective of wind power output variability, Int. J. Climatol. (2015), https://doi.org/10.1002/joc.4161.
[13] T.P. Chang, Estimation of wind energy potential using different probability density functions, Appl. Energy (2011), https://doi.org/10.1016/j.apenergy.2010.11.010.
[14] S.H. Pishgar-Komleh, A. Keyhani, P. Sefeedpari, Wind speed and power density analysis based on Weibull and Rayleigh distributions (a case study: firouzkooh county of Iran), Renew. Sustain. Energy Rev. (2015), https://doi.org/10.1016/j.rser.2014.10.028.
[15] P. Wais, A review of Weibull functions in wind sector, Renew. Sustain. Energy Rev. (2017), https://doi.org/10.1016/j.rser.2016.12.014.
[16] J.A. Carta, P. Ramirez, S. Velazquez, A review of wind speed probability distributions used in wind energy analysis: case studies in the Canary Islands, Renew. Sustain. Energy Rev. 13 (5) (2009) 933–955.
[17] V.L. Brano, A. Orioli, G. Ciulla, S. Culotta, Quality of wind speed fitting distributions for the urban area of Palermo, Ital. Renew. Energy (2011), https://doi.org/10.1016/j.renene.2010.09.009.
[18] N. Aries, S.M. Boudia, H. Ounis, Deep assessment of wind speed distribution models: a case study of four sites in Algeria, Energy Convers. Manag. (2018), https://doi.org/10.1016/j.enconman.2017.10.082.
[19] H. Ounis, N. Aries, On the wind resource in Algeria: probability distributions evaluation, Proc. IME J. Power Energy (2021), https://doi.org/10.1177/0957650920975883.
[20] M.A. Saeed, Z. Ahmed, W. Zhang, Wind Energy Potential and Economic Analysis with a Comparison of Different Methods for Determining the Optimal Distribution Parameters, Renewable Energy, 2020, https://doi.org/10.1016/j.renene.2020.07.064.
[21] P.K. Sharma, A. Gautam, V. Warudkar, S. Ahmed, J.L. Bhagoria, Analysis of Wind Characteristics Parameters with the Application of Lidar and Mast, Wind Energy, 2021, https://doi.org/10.1002/we.2580.
[22] A.N. Celik, A Statistical Analysis of Wind Power Density Based on the Weibull and Rayleigh Models at the Southern Region of Turkey, Renewable Energy, 2004, https://doi.org/10.1016/j.renene.2003.07.002.
[23] D. Cousineau, Fitting the three-parameter weibull distribution: review and evaluation of existing and new methods, IEEE Trans. Dielectr. Electr. Insul. (2009), https://doi.org/10.1109/TDEI.2009.4784578.
[24] S.A. Akdağ, H.S. Bagiorgas, G. Mihalakakou, Use of two-component Weibull mixtures in the analysis of wind speed in the Eastern Mediterranean, Appl. Energy (2010), https://doi.org/10.1016/j.apenergy.2010.02.033.
[25] A.J. Collados-Lara, S.R. Fassnacht, E. Pardo-Igúzquiza, D. Pulido-Velazquez, Assessment of high resolution air temperature fields at rocky mountain national park by combining scarce point measurements with elevation and remote sensing data, Rem. Sens. (2021), https://doi.org/10.3390/rs13010113.
[26] F. González-Longatt, H. Medina, J. Serrano González, Spatial interpolation and orographic correction to estimate wind energy resource in Venezuela, Renew. Sustain. Energy Rev. (2015), https://doi.org/10.1016/j.rser.2015.03.042.
[27] A.J. Collados-Lara, E. Pardo-Igúzquiza, D. Pulido-Velazquez, Spatiotemporal estimation of snow depth using point data from snow stakes, digital terrain models, and satellite data, Hydrol. Process. (2017), https://doi.org/10.1002/hyp.11165.
[28] A.J. Collados-Lara, D. Pulido-Velazquez, E. Pardo-Igúzquiza, E. Alonso-González, Estimation of the spatiotemporal dynamic of snow water equivalent at mountain range scale under data scarcity, Sci. Total Environ. (2020), https://doi.org/10.1016/j.scitotenv.2020.140485.
[29] A.J. Collados-Lara, E. Pardo-Igúzquiza, D. Pulido-Velazquez, J. Jiménez-Sánchez, Precipitation fields in an alpine Mediterranean catchment: inversion of precipitation gradient with elevation or undercatch of snowfall? Int. J. Climatol. (2018) https://doi.org/10.1002/joc.5517.
[30] P. Jimeno-Sáez, D. Pulido-Velazquez, A.J. Collados-Lara, E. Pardo-Igúzquiza, J. Senent-Aparicio, L. Baena-Ruiz, A preliminary assessment of the "undercatching" and the precipitation pattern in an alpine basin, Water (Switzerland) (2020), https://doi.org/10.3390/W12041061.
[31] S. Van Ackere, G. Van Eetvelde, D. Schillebeeckx, E. Papa, K. Van Wyngene, L. Vandevelde, Wind resource mapping using landscape roughness and spatial interpolation methods, Energies (2015), https://doi.org/10.3390/en8088682.
[32] M. Cellura, G. Cirrincione, A. Marvuglia, A. Miraoui, Wind Speed Spatial Estimation for Energy Planning in Sicily: Introduction and Statistical Analysis, Renewable Energy, 2008, https://doi.org/10.1016/j.renene.2007.08.012.
[33] J.P. Chilès, P. Delfiner, Geostatistics, Modeling Spatial Uncertainty, Wiley, 1999.
[34] J.F. Manwell, J.G. McGowan, A.L. Rogers, Wind energy explained: theory, design and application, Wind Energy Explain.: Theory Des Appl. (2010), https://doi.org/10.1002/9781119994367.
[35] J. Silva, C. Ribeiro, R. Guedes, Roughness length classification of corine land cover classes, in: European Wind Energy Conference and Exhibition 2007, 2007. EWEC 2007.
[36] J. Yan, C. Möhrlen, T. Göçmen, M. Kelly, A. Wessel, G. Giebel, Uncovering wind power forecasting uncertainty sources and their propagation through the whole modelling chain, Renew. Sustain. Energy Rev. 165 (2022), 112519.
[37] N. Torbick, D. Lusch, J. Qi, N. Moore, J. Olson, J. Ge, Developing land use/land cover parameterization for climate-land modelling in East Africa, Int. J. Rem. Sens. (2006), https://doi.org/10.1080/01431160600702426.
[38] M. Kelly, H.E. Jørgensen, Statistical characterization of roughness uncertainty and impact on wind resource estimation, Wind Energy Sci. 2 (1) (2017) 189–209.
[39] M. Brower, J.W. Zack, B. Bailey, M.N. Schwartz, D.L. Elliott, Mesoscale Modeling as a Tool for Wind Resource Assessment and Mapping, Bulletin of the American Meteorological Society, 2004.
[40] I. Clark, The art of cross validation in geostatistical application, Proc. 19th APCOM Symp. (1986) 212.
[41] Agencia Andaluza de la Energía (Aae), INFORME DE INFRAESTRUCTURAS ENERGÉTICAS Provincia GRANADA, 2020.
[42] A. Ulazia, J. Sáenz, G. Ibarra-Berastegi, S.J. González-Rojí, S. Carreno-Madinabeitia, Global estimations of wind energy potential considering seasonal air density changes, Energy (2019), https://doi.org/10.1016/j.energy.2019.115938.
[43] A.J. Collados-Lara, S.R. Fassnacht, D. Pulido-Velazquez, A.K.D. Pfohl, E. Morán-Tejeda, N.B.H. Venable, K. Puntenney-Desmond, Intra-day variability of temperature and its near-surface gradient with elevation over mountainous terrain: comparing MODIS land surface temperature data with coarse and fine scale near-surface measurements, Int. J. Climatol. (2021), https://doi.org/10.1002/joc.6778.
[44] B. Jourdier, Evaluation of ERA5, MERRA-2, COSMO-REA6, NEWA and AROME to simulate wind power production over France, Adv. Sci. Res. (2020), https://doi.org/10.5194/asr-17-63-2020.
[45] M. Gross, V. Magar, A. Peña, The effect of averaging, sampling, and time series length on wind power density estimations, Sustainability 12 (2020) 3431, https://doi.org/10.3390/su12083431.
[46] J. Zhou, E. Erdem, G. Li, J. Shi, Comprehensive Evaluation of Wind Speed Distribution Models: A Case Study for North Dakota Sites, Energy Conversion and Management, 2010, https://doi.org/10.1016/j.enconman.2010.01.020.
[47] S. Outten, S. Sobolowski, Extreme Wind Projections over Europe from the Euro-CORDEX Regional Climate Models, Weather and Climate Extremes, 2021, https://doi.org/10.1016/j.wace.2021.100363.